Time-Reversal-Invariant Z_4 Fractional Josephson Effect

Fan Zhang and C. L. Kane
Department of Physics and Astronomy, University of Pennsylvania, Philadelphia, Pennsylvania 19104, USA
(Received 5 April 2014; published 14 July 2014)

We study the Josephson junction mediated by the quantum spin Hall edge states and show that electron-electron interactions lead to a dissipationless fractional Josephson effect in the presence of time-reversal symmetry. Surprisingly, the periodicity is 8π, corresponding to a Josephson frequency $eV/2\hbar$. We estimate the magnitude of interaction-induced many-body level splitting responsible for this effect and argue that it can be measured by using tunneling spectroscopy. For strong interactions we show that the Josephson effect is associated with the weak tunneling of charge $e/2$ quasiparticles between the superconductors. Our theory describes a fourfold ground state degeneracy that is similar to that of coupled "fractional" Majorana modes but is protected by time-reversal symmetry.

DOI: 10.1103/PhysRevLett.113.036401 PACS numbers: 71.10.Pm, 02.40.Pc, 03.65.Vf, 74.50.+r

Topological superconductivity is a topic of current interest because of its potential for providing a method for storing and manipulating quantum information [1–4]. The simplest implementation of this proposal uses the Majorana modes predicted to occur at the end of a 1D topological superconductor. A promising route to achieve this is to employ a proximity effect device that combines an ordinary superconductor with a material that has a single helical band [5–12]. There has been progress towards this goal by using InSb quantum wires [13] and using the edge states of quantum spin Hall (QSH) insulators in HgTe [14] and InAs/GaSb [15] quantum wells.

One of the most basic consequences of topological superconductivity is the fractional Josephson effect [1,6,16–18]. This occurs due to the coherent tunneling of electrons between the Majorana end states of two 1D topological superconductors. A pair of Majorana modes defines two states that are split by the electron tunneling and are distinguished by their local fermion parity. Advancing the phase difference ϕ across the junction by 2π interchanges the two states, which leads to a 4π periodicity for each state as an adiabatic function of ϕ. This resembles a "Z_2 pump" [18,19] and may be referred to as a "Z_2 fractional Josephson effect." It gives rise to an ac Josephson effect with half the conventional Josephson frequency, provided scattering from thermally excited bulk quasiparticles is sufficiently suppressed.

The fractional Josephson effect was originally proposed by Kitaev [1] using a model 1D spinless p wave superconductor. It was later found that similar physics can arise for a Josephson junction mediated by the QSH edge states [6,18]. In this case, a weakly coupled junction is formed by introducing a magnetic gap to the edge states between the superconductors, creating two weakly coupled Majorana modes at the superconductor-magnet interfaces. For this construction it was essential that the time-reversal symmetry (TRS) be explicitly broken in the junction region to produce a dissipationless Josephson effect. If it is not, then the Andreev bound states (ABSs) do not decouple from bulk states, and bulk quasiparticles are necessarily generated as ϕ is adiabatically advanced.

In this Letter, we will show that electron-electron interactions restore the time-reversal-invariant fractional Josephson effect but lead to an 8π periodicity of the Josephson current, which we refer to as a Z_4 fractional Josephson effect. We estimate the magnitude of the interaction-induced splitting in the many-body excitation spectrum and propose a method for detecting this effect by using tunneling spectroscopy. When the QSH edge states between the superconductors are ungapped, the junction is necessarily strongly coupled. However, if the edge states

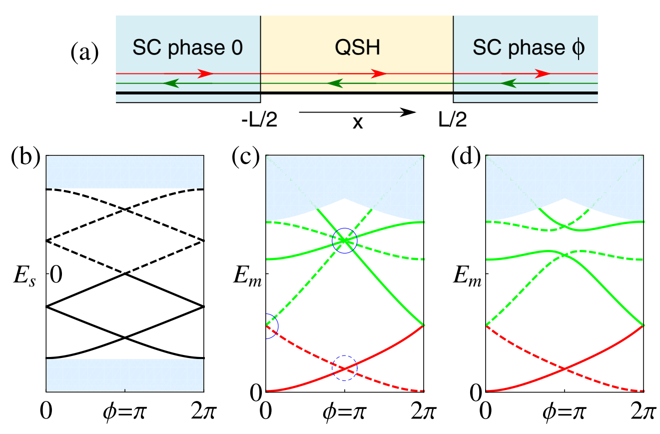

FIG. 1 (color online). (a) The schematic of a Josephson junction mediated by the QSH edge states. (b) The single-particle spectrum E_s of the junction, with Kramers degeneracies at $\phi = 0$ and π. (c) The many-body spectrum E_m associated with (b), including a fourfold degeneracy at $\phi = \pi$. (d) The fourfold degeneracy is lifted by electron-electron interactions, leading to an 8π periodicity of the four lowest states. The solid and dashed lines reflect the PHS in (b) and distinguish opposite fermion parity in (c) and (d).

acquire a gap, we show that the Z_4 Josephson effect is associated with the tunneling of charge $e/2$ quasiparticles. In this weak coupling limit, the junction has a fourfold ground state degeneracy that is lifted with a characteristic pattern by tunneling. The interface between the gapped edge states and the superconductor exhibits a domain wall excitation, which is analogous to the "fractional" Majorana mode [20–26] and related to a Z_4 parafermion. However, there are also important differences with the parafermion theory, which we will clarify.

We begin with the model for a Josephson junction at the edge of a QSH insulator [6], described by the Bogoliubov–de Gennes Hamiltonian

$$\mathcal{H}_{\rm BdG} = \tau^z(-i\hbar v_F \sigma^z \partial_x - \mu) + \Delta_1(x)\tau^x + \Delta_2(x)\tau^y, \qquad (1)$$

where $\vec{\sigma}$ ($\vec{\tau}$) are Pauli matrices in spin (particle-hole) space and $\Delta = \Delta_1 + i\Delta_2$ is the proximity-induced pair potential. We suppose that $\Delta(x < -L/2) = \Delta_0$, $\Delta(x > L/2) = \Delta_0 e^{i\phi}$, and $\Delta(|x| < L/2) = 0$. The single-particle spectrum is shown in Fig. 1(b). The ABSs at the phase difference $\phi = 0$ and π are necessarily Kramers degenerate. This leads to a breakdown of the ac Josephson effect, because as ϕ advances quasiparticles pass through the Kramers degeneracies and end up above the bulk gap leading to dissipation.

To go beyond the model where the junction is noninteracting, we consider in Fig. 1(c) the many-body spectrum associated with Fig. 1(b). The lowest state in Fig. 1(c) corresponds to the many-body ground state with all positive (negative) energy single-particle states in Fig. 1(b) empty (occupied), whereas higher states are excitations with one or more quasiparticles excited, taking into account the intrinsic particle-hole symmetry (PHS) in Fig. 1(b). The local fermion parity of each many-body state is indicated by the solid and dashed lines, and due to the fermion parity anomaly their identity switches when ϕ advances by 2π. Figure 1(c) exhibits several degeneracies. The twofold degeneracies at $\phi = 0$ and π are Kramers degeneracies, protected by TRS. The twofold degeneracy at $\phi = \pi$ labeled by an open circle is even robust against TRS breaking, since it involves two states with opposite fermion parity. The fourfold degeneracy at $\phi = \pi$ labeled by a solid circle reflects the degeneracies of both $E = 0$ and $E \neq 0$ single-particle states. However, this fourfold degeneracy is an artifact of the noninteracting electron approximation. In the presence of electron-electron interactions, it splits into two Kramers doublets, each of which has two many-body states with opposite fermion parity. There are thus only four low-energy states that mix among themselves as ϕ is adiabatically advanced, as indicated in Fig. 1(d). Starting from the ground state at $\phi = 0$, it takes four cycles to return to the original ground state, leading to an 8π periodicity in the current phase relation. In the presence of a bias voltage V, this leads to an ac Josephson effect with a fundamental frequency $\omega_J = eV/2\hbar$, i.e., one-quarter of the conventional Josephson frequency.

To establish the splitting at $\phi = \pi$ and estimate its magnitude, we introduce a model $\mathcal{H} = \mathcal{H}_0 + \mathcal{H}_I$, where $\mathcal{H}_0$ is a second quantized version of Eq. (1) and

$$\mathcal{H}_I = \lambda \int_{-L/2}^{L/2} n(x)^2. \qquad (2)$$

Here $n(x) = \sum_\sigma c^\dagger_\sigma c_\sigma$ is the charge density. We focus on the four degenerate excited states at $\phi = \pi$ and evaluate the splitting to first order in λ. To proceed, we now determine the wave functions of single-particle ABSs and then evaluate the matrix elements of $\mathcal{H}_I$ between the degenerate many-body states.

The single-particle ABSs are found by solving Eq. (1) subject to the appropriate matching conditions at $x = \pm L/2$. For $\phi = \pi$, the energy eigenstates are Kramers pairs $\psi_{n,\sigma}$ indexed by $\sigma = \pm 1$, the eigenvalues of σ_z. The energy eigenvalues E_n satisfy

$$\tan \bar{E}_n \bar{L} = -\bar{E}_n (1 - \bar{E}_n^2)^{-1/2}, \qquad (3)$$

where the bars denote dimensionless quantities $\bar{E}_n \equiv E_n/\Delta_0$ and $\bar{L} \equiv L/\xi = L\Delta_0/\hbar v_F$. For $-\pi < 2(\bar{L} - N\pi) \leq \pi$, there are N pairs of ABSs in addition to the Majorana Kramers pair at $E_0 = 0$. The wave functions $\psi_{n,\sigma} = (u_{n,\sigma}, v_{n,\sigma})^T$ with $E_n \geq 0$ are

$$\begin{pmatrix} u_{n,\sigma} \\ v_{n,\sigma} \end{pmatrix} = \mathcal{A}_n e^{i\sigma\bar{\mu}\bar{x} - \sqrt{1-\bar{E}_n^2}|\bar{x} - \bar{\ell}(x)|} \begin{pmatrix} (-1)^n e^{i\sigma\bar{E}_n\bar{\ell}(x)} \\ -i\sigma e^{-i\sigma\bar{E}_n\bar{\ell}(x)} \end{pmatrix}, \qquad (4)$$

where $\bar{\ell}(x)$ is x/ξ for $|x| < L/2$ and $\mathrm{sgn}(x)\bar{L}/2$ for $|x| > L/2$. The normalization factor satisfies

$$\mathcal{A}_n^{-2} = 2L + 2\xi(1 - \bar{E}_n^2)^{-1/2}. \qquad (5)$$

PHS and TRS imply that states with $E_{-n} = -E_n$ are related by $\psi_{-n,\sigma} = -i\tau^y \psi_{n,\sigma}$ ($n > 0$). The corresponding second quantized operators obey $b_{-n,\sigma} = \sigma b^\dagger_{n,-\sigma}$ ($n > 0$) and $b_{0,+} = i b^\dagger_{0,-}$. It follows that the electron annihilation operator may be written as

$$c_\sigma(x) = u_{0,\sigma} b_{0,\sigma} + \sum_{n>0} u_{n,\sigma} b_{n,\sigma} - v_{n,\sigma} \sigma b^\dagger_{n,-\sigma}. \qquad (6)$$

We assume $\bar{L} > \pi/2$ so that there is at least one pair of excited ($E_s \neq 0$) ABSs at $\phi = \pi$. The four degenerate many-body states are $|\mu, \sigma\rangle = b^\dagger_{1,\sigma}|\mu\rangle_0$, where $|\mu\rangle_0$ is the many-body ground state with $b^\dagger_{n,\sigma} b_{n,\sigma} = 0$ ($n > 0$) and $(-1)^{b^\dagger_{0,+} b_{0,+}} = \mu$. For these four states $\mu = \pm 1$, the eigenvalues of μ^z, distinguishes states with different fermion parity. Under time reversal [27], $\Theta|\mu, \sigma\rangle = \sigma|-\mu, -\sigma\rangle$ and Θ may be represented by $\mu^x \sigma^y K$. The most general interaction consistent with TRS and fermion parity conservation then has the form $h_I = m_0 + \vec{m} \cdot \vec{\sigma} \mu^z$ [28]. This splits the four states into two Kramers pairs with $E = m_0 \pm |\vec{m}|$.

By plugging Eqs. (4) and (6) into the density-density interactions (2), we find that $m_x = m_y = 0$ and

$$2m_z = \frac{\lambda}{\xi}\left(\frac{1}{\sqrt{1-\bar{E}_1^2}} + \bar{L}\right)^{-1}. \quad (7)$$

When $\bar{L} \sim 2.6$, the level splitting at $\phi = \pi$ can reach its largest amplitude $2m_z \sim 0.23\lambda/\xi$. Physically, $\lambda = (e^2/\epsilon)\log(R_s/R)$, where ϵ is the dielectric constant; R and R_s are, respectively, the penetration length and the screening radius of the edge states. For $\epsilon = 20$, $\xi = 100$ nm, and $\log(R_s/R) = 1$, the splitting can reach 0.17 meV, which is comparable to Δ_0. We also note that, in the presence of impurities, TRS allows scattering such as $(c_\uparrow^\dagger c_\uparrow c_\downarrow^\dagger \partial_x c_\uparrow - c_\downarrow^\dagger c_\downarrow c_\uparrow^\dagger \partial_x c_\downarrow) + \mathrm{H.c.}$, yielding to nonzero $m_{x,y}$. Estimating $m_{x,y}$ is beyond the scope here, and we assume that they are in the same order of m_z.

Observing the fractional Josephson effect is complicated by scattering from thermally excited bulk quasiparticles, which can cause the system to relax to the ground state before a cycle is completed. It has been suggested that qualitative features of the Z_2 Josephson effect remain for equilibrium critical current measurements [29]. Here we consider a different method to demonstrate the Z_4 Josephson effect by probing the phase dependence of the tunneling spectrum of ABSs at the junction.

Consider a ring geometry where the phase difference ϕ across the junction is controlled by a weak applied magnetic field. We propose tunneling into the junction region by using an additional tunnel contact to probe the discrete many-body excitation spectrum. This approach has been successfully used [30,31] to probe the ABSs of 1D superconductor-nanowire-superconductor junctions in similar geometries. At low temperature, a weakly coupled tunnel junction probes the local tunneling density of states (DOS), $dI/dV \propto \rho(E_t = eV)$ with

$$\rho(E_t) = \sum_{N,\sigma} |\langle N|c_\sigma^\dagger|0\rangle|^2 \delta(E_t - E_m^N + E_m^0), \quad (8)$$

where $c_\sigma^\dagger$ is the creation operator for an electron with spin σ and $|N\rangle$ are the many-body states at energy E_m^N in Fig. 1(d). Importantly, there is a selection rule dictating that the excited state $|N\rangle$ must have the opposite fermion parity from the ground state $|0\rangle$.

In Fig. 2, we plot the zero temperature peaks in the tunneling DOS based on the spectra in Fig. 1. dI/dV must consist of peaks at $eV = E_m^N - E_m^0$. Figure 2(a) shows the tunneling spectrum in the noninteracting electron approximation. Figure 2(b) shows the spectrum when electron-electron interactions eliminate the many-body degeneracies. Figure 2(c) shows the qualitative spectrum when TRS is strongly broken. There are four important features. (i) Figures 2(a)–2(c) all share a singularity in which the lowest peak goes to zero. This is a consequence of the Z_2 Josephson effect, which requires a level crossing in the ground state when ϕ is advanced by 2π. Since this crossing changes the fermion parity, it is visible in tunneling spectroscopy. TRS fixes this singularity at $\phi = \pi$, whereas with broken TRS it can shift. (ii) In the higher excited levels, similar singularities persist even with interactions, whereas with broken TRS they may disappear. (iii) Figure 2(a) exhibits a degeneracy in the tunneling peaks at $\phi = \pi$, which is split in Fig. 2(b) by $2m_z$ in Eq. (7) due to interactions. (iv) Figures 2(a) and 2(b) both have the same Kramers degeneracy in the lowest two peaks at $\phi = 0$, which is lifted in Fig. 2(c) where TRS is broken. Taken together, these four features would provide compelling evidence for the excitation spectrum responsible for the Z_4 Josephson effect.

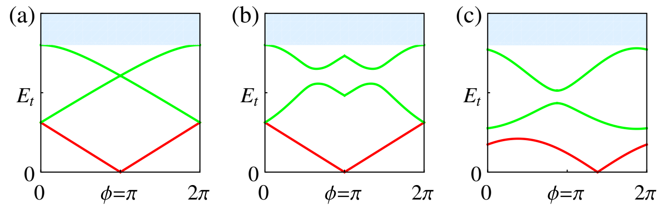

FIG. 2 (color online). Phase dependence of the energies of peaks in the tunneling DOS. In the noninteracting case, (a) shows a degeneracy at $\phi = \pi$ that is lifted in (b) by interactions. Breaking TRS lifts both degeneracies in (a), as shown in (c).

The presence of a weak magnetic field that controls ϕ will break TRS and split the Kramers degeneracies. The magnitude of the Zeeman splitting is $E_Z \sim g\mu_B B$. Using $g \leq 1$ appropriate for the QSH edge states [32,33], we find $E_Z \leq 0.058 \times B[T]$ meV, which is negligible for $B < 10$ mT relevant for the related experiments.

The Z_2 fractional Josephson effect can be understood in a weak coupling limit in which an electron—or half a Cooper pair—coherently tunnels between two Majorana bound states. It is natural to ask whether there is a similar weak coupling version of the time-reversal-invariant Z_4 fractional Josephson effect. For weak interactions, this is not possible, because TRS prevents an energy gap from opening in the QSH edge state between the superconductors. However, strong interactions can lead to an energy gap [34,35]. We now show that in this case the Josephson effect is mediated by the tunneling of charge $e/2$ quasiparticles. The domain wall at the interface between the gapped edge state and the superconductor behaves as a "fractional" Majorana mode, which is related to a Z_4 parafermion.

To describe the QSH edge state with strong interactions, we adopt a bosonized representation in which the electron creation operators are $c_{R\uparrow(L\downarrow)}^\dagger \propto e^{i(\varphi\pm\theta)}$ and the bosonic variables satisfy $[\varphi(x), \theta(x')] = i\pi\Theta(x - x')$. TRS forbids the single-particle backscattering term $\cos 2\theta$, which would lead to a magnetic energy gap. However, the *pair* backscattering term $\cos 4\theta$ respects TRS and will be present—either as a momentum-conserving process if $\mu = 0$ or as an impurity scattering process. We thus consider the

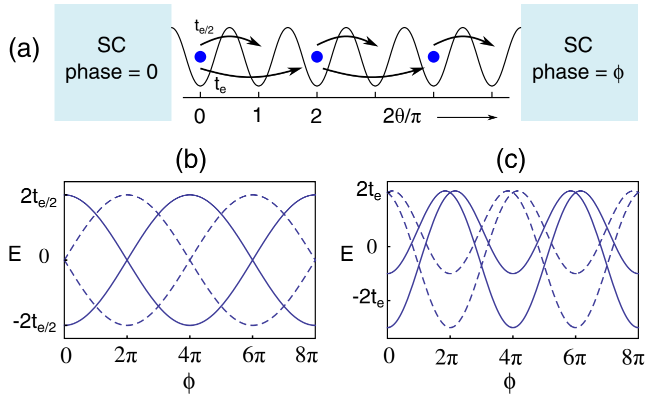

FIG. 3 (color online). (a) Strong interactions pin the charge between the superconductors and lead to a fourfold ground state degeneracy. Charge $e/2$ or charge e tunneling processes lift the degeneracy, with an 8π periodicity in ϕ, as shown in (b) for $t_e = 0$ and (c) for $t_e = 2t_{e/2}$. Solid and dashed lines correspond to states with opposite fermion parity.

Hamiltonian $\mathcal{H} = \mathcal{H}_0 + \mathcal{H}_I + \mathcal{H}_\theta + \mathcal{H}_\varphi$ for the QSH edge state, where

$$\mathcal{H}_0 + \mathcal{H}_I = \frac{v_F}{2\pi}[(\partial_x\theta)^2 + (\partial_x\varphi)^2] + \frac{\lambda(x)}{\pi^2}(\partial_x\theta)^2, \quad (9)$$

with $\lambda(x) = \lambda\Theta(|x| - L/2)$. The superconducting proximity effect and the pair backscattering are described by

$$\mathcal{H}_\varphi = u_0\left[\Theta\left(-\frac{L}{2} - x\right)\cos 2\varphi + \Theta\left(x - \frac{L}{2}\right)\cos(2\varphi - \phi)\right],$$
$$\mathcal{H}_\theta = v_0\Theta\left(\frac{L}{2} - |x|\right)\cos 4\theta. \quad (10)$$

$\mathcal{H}_\varphi$ introduces a superconducting energy gap into the QSH edge states coupled to the superconductors. For weak interactions $\mathcal{H}_\theta$ is irrelevant, but $\mathcal{H}_\theta$ will flow to strong coupling and open a gap for $\lambda > 4.7v_F$ for $\mu = 0$ (corresponding to Luttinger parameter $g < 1/2$). For impurity scattering, states are localized for $\lambda > 9.6v_F$ $(g < 3/8)$ [36]. It is simplest to analyze the large v_0 limit, where θ is pinned in the deep wells of the cosine potential, depicted in Fig. 3(a). This describes a magnetic state that spontaneously breaks TRS. The presence of the $\cos 2\varphi$ introduces 2π jumps in θ that effectively make θ an angular variable defined modulo 2π, reflecting the condensation of Cooper pairs. There are thus four distinct minima of the $\cos 4\theta$ potential leading to a fourfold degenerate ground state for the junction. When v_0 is finite, quantum tunneling between the minima will couple the four states, lifting their degeneracy with a characteristic pattern. A tunneling event from $\theta = n\pi/2$ to $\theta = (n+1)\pi/2$ can be interpreted as the tunneling of a domain wall between the two degenerate magnetic states, which is associated with a charge $e/2$ [37–39]. This has the effect of flipping the magnetization of the junction region while transferring a charge $e/2$.

If $|n\rangle$ denotes the state $\theta = n\pi/2$ (with n defined modulo 4), the Hamiltonian in the degenerate subspace is

$$H = \sum_{n=1}^{4}(-t_{e/2}e^{i(\phi/4)}|n\rangle\langle n+1| - t_e e^{i(\phi/2)}|n\rangle\langle n+2| + \mathrm{H.c.}), \quad (11)$$

with an energy spectrum $E_{m=1,2,3,4} = -2t_{e/2}\cos[(\phi - 2\pi m)/4] - 2t_e\cos[(\phi - 2\pi m)/2]$. Here $t_{e/2}$ is the amplitude for tunneling a single $e/2$ quasiparticle, whereas t_e is the amplitude for tunneling charge e. In general, there will also be a contribution from tunneling charge $2e$ Cooper pairs across the junction, which only gives an overall ϕ-dependent shift to all four energy levels. In Figs. 3(b) and 3(c), we show $E_m(\phi)$ in the cases where tunnelings are dominated by $t_e = 0$ and $t_e = 2t_{e/2}$, respectively. They share a pattern of fermion parity degeneracies (at $\phi = \pi$) and Kramers degeneracies (at $\phi = 0$) that guarantee an 8π periodicity when ϕ is advanced adiabatically. The tunneling DOS features in Fig. 2(b) also apply here.

Equation (10) is similar to models that have recently been introduced to describe "fractional" Majorana modes in superconductor–fractional quantum Hall insulator structures [20–26]. These models share competing terms $\cos p\theta$ and $\cos 2\varphi$ with Eq. (10), analogous to the order and disorder variables of a Z_p clock model [40]. For $p = 3$, the critical point of the Z_3 clock model is described by the Z_3 parafermion conformal field theory [41]. In this case, an interface between regions dominated by $\cos p\theta$ and by $\cos 2\varphi$ binds a local Z_3 parafermion, which is related via a similar construction [42] to the quasiparticles of the Read-Rezayi state [43]. The $p = 4$ case of interest here is slightly different. The Z_4 clock model and the Z_4 parafermion model are not equivalent but are rather two different points in the more general Ashkin-Teller model. Nonetheless, the domain wall defines an excitation similar to a Z_4 parafermion, and a pair of such defects encodes a fourfold degeneracy. The domain walls that occur in superconductors coupled to fractionalized states with charge e/m quasiparticles involve a similar Z_{2m} clock model (which also differs from the parafermion model) and lead to a Z_{2m} fractional Josephson effect. Despite the mathematical similarity, there is an important difference between Eq. (10) and the models based on fractionalized states [20–26]. In the latter case, the ground state degeneracy defined by a pair of domain walls is a *topological* degeneracy that cannot be lifted by any local perturbation. By contrast, half of the fourfold degeneracy defined by the Josephson junction here is a *local* degeneracy that can be lifted by a Zeeman field $h\cos 2\theta$. In Fig. 3, this eliminates the crossings between states with the same parity. The fourfold degeneracy here, however, is a *symmetry-protected* degeneracy that is guaranteed as long as TRS is not violated.

We thank Jeffrey Teo for helpful discussions. This work was supported by DARPA SPAWAR Grant No. N66001-11-1-4110 and a Simons Investigator award to C. L. K. from the Simons Foundation.

[1] A. Kitaev, Sov. Phys. Usp. **44**, 131 (2001).
[2] J. Alicea, Rep. Prog. Phys. **75**, 076501 (2012).
[3] C. Beenakker, Annu. Rev. Condens. Matter Phys. **4**, 113 (2013).
[4] P. Wiegmann, Prog. Theor. Phys. Suppl. **107**, 243 (1992). While the term topological superconductivity was used in this reference to describe a mechanism of superconductivity based on a topological order (condensation of charged Skyrmions), our use of the term follows Refs. [2,3].
[5] L. Fu and C. L. Kane, Phys. Rev. Lett. **100**, 096407 (2008).
[6] L. Fu and C. L. Kane, Phys. Rev. B **79**, 161408(R) (2009).
[7] J. Nilsson, A. R. Akhmerov, and C. W. J. Beenakker, Phys. Rev. Lett. **101**, 120403 (2008).
[8] M. Sato, Y. Takahashi, and S. Fujimoto, Phys. Rev. Lett. **103**, 020401 (2009).
[9] J. D. Sau, R. M. Lutchyn, S. Tewari, and S. Das Sarma, Phys. Rev. Lett. **104**, 040502 (2010).
[10] J. Alicea, Phys. Rev. B **81**, 125318 (2010).
[11] R. M. Lutchyn, J. D. Sau, and S. Das Sarma, Phys. Rev. Lett. **105**, 077001 (2010).
[12] Y. Oreg, G. Refael, and F. von Oppen, Phys. Rev. Lett. **105**, 177002 (2010).
[13] V. Mourik, K. Zuo, S. M. Frolov, S. R. Plissard, E. P. A. M. Bakkers, and L. P. Kouwenhoven, Science **336**, 1003 (2012).
[14] S. Hart, H. Ren, T. Wagner, P. Leubner, M. Mühlbauer, C. Brüne, H. Buhmann, L. W. Molenkamp, and A. Yacoby, arXiv:1312.2559.
[15] I. Knez, R. R. Du, and G. Sullivan, Phys. Rev. Lett. **109**, 186603 (2012).
[16] H. J. Kwon, K. Sengupta, and V. M. Yakovenko, Eur. Phys. J. B **37**, 349 (2004).
[17] F. S. Nogueira and I. Eremin, J. Phys. Condens. Matter **24**, 325701 (2012).
[18] F. Zhang and C. L. Kane, Phys. Rev. B **90**, 020501(R) (2014).
[19] L. Fu and C. L. Kane, Phys. Rev. B **74**, 195312(R) (2006).
[20] M. Barkeshli and X. L. Qi, Phys. Rev. X **2**, 031013 (2012).
[21] D. J. Clarke, J. Alicea, and K. Shtengel, Nat. Commun. **4**, 1348 (2013).
[22] N. H. Lindner, E. Berg, G. Refael, and A. Stern, Phys. Rev. X **2**, 041002 (2012).
[23] M. Cheng, Phys. Rev. B **86**, 195126 (2012).
[24] A. Vaezi, Phys. Rev. B **87**, 035132 (2013).
[25] R. S. K. Mong, D. J. Clarke, J. Alicea, N. H. Lindner, P. Fendley, C. Nayak, Y. Oreg, A. Stern, E. Berg, K. Shtengel, and M. P. A. Fisher, Phys. Rev. X **4**, 011036 (2014).
[26] J. Klinovaja and D. Loss, Phys. Rev. Lett. **112**, 246403 (2014); J. Klinovaja, A. Yacoby, and D. Loss, arXiv:1403.4125.
[27] In the 0D space here, the time-reversal symmetry acts like a supersymmetry that flips the fermion parity. This is similar to the case in F. Zhang, C. L. Kane, and E. J. Mele, Phys. Rev. Lett. **111**, 056402 (2013).
[28] These are the symmetry-allowed interactions between the Majorana fermions at $E = 0$ and the ABSs at E_1 in Fig. 1(b). Thus, their energy difference E_1 appears in Eq. (7).
[29] S. P. Lee, K. Michaeli, J. Alicea, and A. Yacoby, arXiv:1403.2747.
[30] J.-D. Pillet, C. H. L. Quay, P. Morfin, C. Bena, A. Levy Yeyati, and P. Joyez, Nat. Phys. **6**, 965 (2010).
[31] H. le Sueur, P. Joyez, H. Pothier, C. Urbina, and D. Esteve, Phys. Rev. Lett. **100**, 197002 (2008).
[32] F. Zhang, C. L. Kane, and E. J. Mele, Phys. Rev. Lett. **110**, 046404 (2013).
[33] L. Du, I. Knez, G. Sullivan, and R. R. Du, arXiv:1306.1925.
[34] C. Wu, B. A. Bernevig, and S. C. Zhang, Phys. Rev. Lett. **96**, 106401 (2006).
[35] C. Xu and J. E. Moore, Phys. Rev. B **73**, 045322 (2006).
[36] T. Giamarchi and H. J. Schulz, Phys. Rev. B **37**, 325 (1988).
[37] W. P. Su, J. R. Schrieffer, and A. J. Heeger, Phys. Rev. Lett. **42**, 1698 (1979).
[38] X. L. Qi, T. L. Hughes, and S. C. Zhang, Nat. Phys. **4**, 273 (2008).
[39] J. Klinovaja, P. Stano, and D. Loss, Phys. Rev. Lett. **109**, 236801 (2012).
[40] E. H. Fradkin and L. P. Kadanoff, Nucl. Phys. **B170**, 1 (1980).
[41] A. B. Zamolodchikov and V. A. Fateev, Sov. Phys. JETP **62**, 215 (1985).
[42] J. C. Y. Teo and C. L. Kane, Phys. Rev. B **89**, 085101 (2014).
[43] N. Read and E. Rezayi, Phys. Rev. B **59**, 8084 (1999).